*Egypt. J. Chem.* **Vol. 67**, No. 8 pp. 179 - 185 (2024)

**Egyptian Journal of Chemistry**

**http://ejchem.journals.ekb.eg/**

# Characterization, optimization, and physicochemical characteristics of polyvinyl alcohol containing sulfa drug

**A.M. Abdelghany[1], I. S. Elashmawi[*,1] Sohier M. Abobakr[2], M.M. Hegazi[3], Zeinab S. Abouelnaga[4]**

*[1]Spectroscopy Department, Physics Research Institute, National Research Centre, ElBehouth St., 12311, Dokki, Giza, Egypt*

*[2]Higher Institute of Engineering and Technology, New Damietta, 34517, Egypt*

*[3]Department of Basic Science, Mansoura Higher Institute of Engineering and Technology, Mansoura, Egypt*

*[4]Zoology Department, Faculty of Science, Mansoura University, 35516, Mansoura, Egypt*

**Abstract**

A new sulfonamide adduct of vitamin C has been created to improve the structural and optical properties of polyvinyl alcohol (PVA) films. PVA films containing different concentrations of sulfa drugs have been prepared and characterized using FT-IR and UV-Vis spectroscopy. The FT-IR absorption spectrum of pure PVA polymer shows characteristic bands related to the functional groups present in the PVA polymer. The FT-IR data demonstrated strong chemical interactions between the functional groups within the hybrid PVA. The FT-IR spectra of PVA films containing sulfa drugs confirmed the presence of the drug in the polymer matrix. The drug-specific bands, such as the sulfonamide group ($SO_2NH_2$), were observed. The intensity of these bands can be used to estimate the drug loading efficiency and drug content in the PVA films. The UV-vis spectra mainly characterized the optical properties of the hybrid film. The extinction coefficient (k) values were significantly elevated. The direct and indirect electronic transition between the valence band and conduction band was determined using Tauc's model. Based on these preliminary results, the flexible composite has great potential for use in antibacterial applications.

**Keywords:** PVA; Sulfa Drug; FT-IR; Optical Properties; hazardous pollutants; environment.

## 1. Introduction

Polyvinyl alcohol (PVA) is a water-soluble polymer that is widely used in various applications because of its excellent film-forming and adhesive properties, biocompatibility, and low toxicity [1-3]. In recent years, drug delivery systems using PVA as a carrier have gained attention due to its biocompatibility and ease of production. Sulfonamide antibiotics, commonly known as sulfa drugs, are a class of drugs used in the treatment of bacterial infections. Incorporating sulfa drugs into PVA films can be a promising strategy for drug delivery applications [4-6].

The physicochemical characteristics of PVA films containing sulfa drugs can be studied using various techniques. The morphology and surface properties of the films can be analyzed using scanning electron microscopy (SEM) and atomic force microscopy (AFM). The presence of sulfa drugs in the PVA matrix can be confirmed using Fourier-transform infrared spectroscopy (FT-IR) and X-ray diffraction (XRD).

The release profile of sulfa drugs from PVA films can be evaluated using various methods such as FT-IR and UV-Vis spectroscopy. The release kinetics of the drug from the PVA matrix can be analyzed using mathematical models such as zero-order and first-order [7, 8]. These analytical techniques can also

*Corresponding author e-mail: islam_shukri2000@yahoo.com

Received date 13 June 2023; revised date 21 July 2023; accepted date 31 July 2023
DOI: 10.21608/EJCHEM.2023.217364.8134

determine the drug loading efficiency and drug content in the PVA films. Sulfonamide, also known as sulfa drugs, is a group of synthetic antibiotics that were first developed in the 1930s. They work by inhibiting the growth and reproduction of bacteria and are used to treat a wide variety of bacterial infections [9-11]. Sulfonamides were some of the first antibiotics to be discovered and were widely used before the development of penicillin. They are still used today, although newer, more effective antibiotics have largely replaced them with fewer side effects [12-14].

Some examples of sulfonamide antibiotics include sulfamethoxazole, sulfadiazine, and sulfisoxazole. These drugs are commonly used to treat urinary tract infections, pneumonia, and other bacterial infections [14, 16]. However, like all antibiotics, sulfonamides can have side effects, including allergic reactions, skin rashes, and gastrointestinal problems. It's important to use antibiotics only as prescribed by a healthcare professional and to complete the full course of treatment to avoid the development of antibiotic-resistant bacteria. Environmentally, it has an obvious ecotoxicological impact on aquatic life and may cause genotoxicity to the fish tissue. This means that even at low concentrations, certain sulfa drugs will alter fish physiology and genetics, even if they do not affect fish survival [17].The physicochemical properties of PVA films containing sulfa drugs can be optimized by varying the concentration of PVA, sulfa drugs, and other additives such as plasticizers and surfactants [18-20]. The mechanical properties of the films can be improved by adding plasticizers such as glycerol and polyethylene glycol.

PVA films containing sulfa drugs have potential applications in drug delivery systems. The physicochemical properties of the films can be optimized by varying the concentration of PVA, sulfa drugs, plasticizers, and surfactants [21-23]. This study's primary objective is to optimize concentrations of sulfa drug within the polymeric matrix, avoiding potential hazardous pollutants in the surrounding environment resulting from the excess amounts of drug within the polymeric matrix. The study extended to characterizing a metal-free sulfonamide-vitamin C adduct utilizing physicochemical characteristics of polyvinyl alcohol-doped matrices containing variable concentrations of the sulfa drug.

## 2. Experimental work

All the chemicals in this article were obtained from Sigma Aldrich Company and used without any purification procedures. PVA films. Sulfonamide, also known as sulfa drugs, is a group of synthetic antibiotics. The procedure involved dissolving 4 g of PVA in 50 mL of double distilled water under mechanical stirring for approximately 2 hours. Subsequently, different concentrations of sulfonamide (0.005 D1, 0.01 D2, 0.02 D3, and 0.04 D4) were added slowly to the solution while stirring for 20 minutes. The resulting solutions were then poured into glass Petri dishes and dried at room temperature for a week, followed by vacuum drying to remove any remaining solvent residue.The FT-IR measurements were conducted using a single-beam FT-IR instrument (FT-IR-430, Jasco, Japan). The spectral range for obtaining the FT-IR spectra of the samples was 4000-400 cm-1. The UV-Vis absorption spectra were obtained using a spectrophotometer (V-570 UV/VIS/NIR, JASCO, Japan) in the 200-1100 nm wavelength range.Antibacterial activity of studied samples against pathogenic *Methicillin-resistant Staphylococcus aureus* (*MRSA*), *Staphylococcus aureus* (*S. aureus*), *Escherichia coli* (*E-coil*), and *Klebsiella pneumonia* (*K*) was performed using disc agar diffusion method. The inhibitory activity was determined based on the diameter of the distinct inhibition district [6].

## 3. Results and discussion

### 3.1. FT-IR spectroscopy

The FT-IR absorption spectra of pure PVA polymer are displayed in Figure 1 in the wavenumber range from 4000-400 $cm^{-1}$. The FT-IR absorption spectra of pure PVA polymer show characteristic bands related to the functional groups present in the polymer. The broad bands centered at 3265 $cm^{-1}$ are attributed to the O-H stretching vibrations from PVA's intermolecular and intramolecular hydrogen bonds. The band at 2916 $cm^{-1}$ corresponds to the asymmetric stretching vibrations of $CH_2$ groups in the alkyl side chains of PVA. The band at 1725 $cm^{-1}$ is due to the stretching vibrations of C=O bonds in the acetate groups present in PVA. The band at 1656 $cm^{-1}$ is attributed to water absorption, while the band at 1420 $cm^{-1}$ corresponds to the $CH_2$ bending vibrations. The band at 1326 $cm^{-1}$ is related to the CH wagging mode, while the band at 1146 $cm^{-1}$ is attributed to the C-O shoulder stretching vibrations of the crystalline sequence of PVA [24-26]. The band at

1081 $cm^{-1}$ corresponds to the C-O stretching and bending vibrations of OH groups in the amorphous sequence of PVA. The band at 919 $cm^{-1}$ is assigned to the $CH_2$ rocking mode, and the band at 840 $cm^{-1}$ is due to the C-C stretching vibrations of the polymer backbone [27, 28].

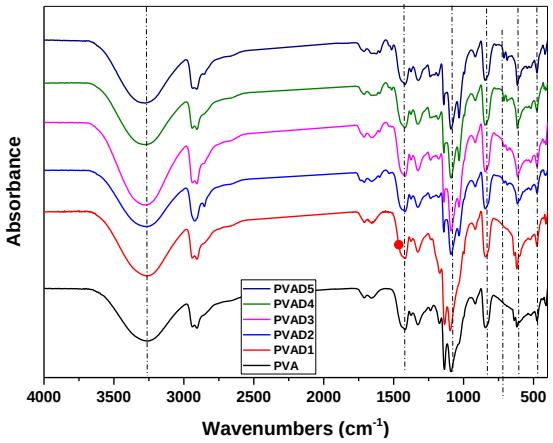


**Figure 1:** The FT-IR absorption spectra of PVA/sulfa drug in the wavenumber range from 4000-400 $cm^{-1}$.

The FT-IR spectra of PVA films containing sulfa drugs can be compared to the spectra of pure PVA to confirm the presence of the drug in the polymer matrix. The drug-specific bands, such as the sulfonamide group ($SO_2NH_2$) at around 1200-1300 $cm^{-1}$ and the aromatic ring bands at around 1600-1700 $cm^{-1}$, can be used to identify the presence of the drug in the PVA matrix [29]. The intensity of these bands can be used to estimate the drug loading efficiency and drug content in the PVA films. Figure (2) introduces the suggested 2D reaction mechanism between PVA polymeric matrix and the dopant sulfa drug through hydrogen bonding of the polyvinyl alcohol matrix.

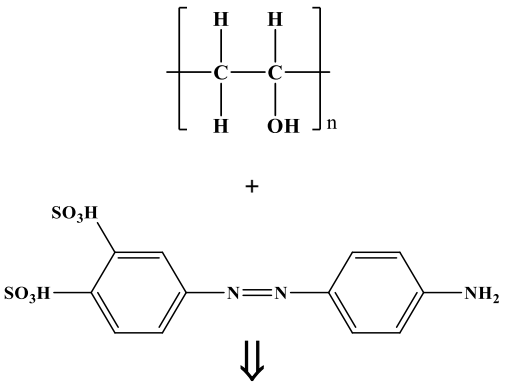


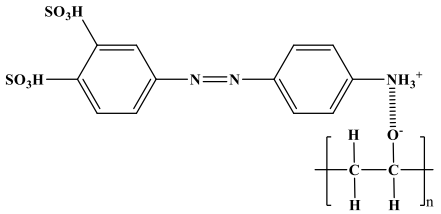


**Figure 2:** suggested 2D reaction mechanism between PVA polymeric matrix and the dopant sulfa drug.

### 3.2. Optical properties

The absorbance spectra of the PVA/sulfa drug in the wavelength range of 190-1100 Hz are depicted in Figure 3. The ultraviolet-visible (UV-Vis) spectrum of pure polyvinyl alcohol (PVA) shows some characteristic absorption bands. Around 198 nm is due to π - π* transition of the -C=O groups in PVA. Though less in number, the carbonyl groups in PVA give rise to absorption in this region. Around 275 nm, the band is due to the n - π* transition of the -C=O groups along with π - π* transition of the benzene rings present in PVA [30]. Shoulder or broad bands observed around 324 nm in this region are due to n - π* transitions of the -OH groups present in PVA. The numerous -OH groups in PVA dominate the UV spectrum in this region. Pure PVA shows very little to no absorption in the visible region above 310 nm. It is mostly transparent to visible light. The number and position of the bands, their relative intensities, and shoulder formations will depend on the molecular weight, degree of polymerization, and other structural features of the specific PVA sample being analyzed. But the general shape and absorption regions discussed above should hold for most pure PVA samples.

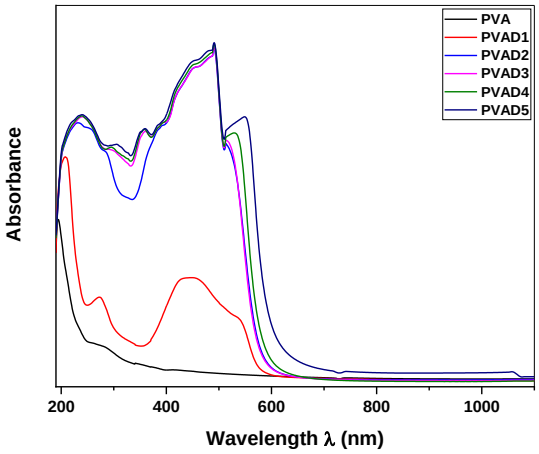


**Figure 3:** The UV-Visible spectra of pure PVA/sulfa drug.

The optical bandgap can be determined from the absorption edge in the UV-Visible spectra. This indicates the π-π* and n-π* excitation energies in PVA related to its carbonyl and hydroxyl groups.

The absorption coefficient (α) of the films can be calculated from its UV-Vis absorption spectrum. The absorption coefficient (α) can be calculated according to the Beer-Lambert Law [31, 32]:

$$\alpha = (2.303A)/d \qquad (1)$$

where d is the thickness of the sample. The value of α indicates how strongly the material absorbs light of that wavelength.

According to the Tauc relation, the optical energy gap ($E_g$) can be calculated as follows[31, 32]:

$$\alpha E_{ph} = A(E_{ph} - E_g)^n \qquad (2)$$

where n refers to the type of electronic transition in the samples.

According to solid-state physics principles, a polymeric material has a specific range of energies known as the "energy gap," where electronic states are not permitted. This results in a lack of absorption of free charge carriers, and interband transitions can only occur with photons that have energies higher than the energy gap.

Figures 4 and 5 display plots of $(\alpha h\upsilon)^2$ and $(\alpha h\upsilon)^{1/2}$ versus photon energy (hυ) for direct and indirect band gap transition. To determine the optical bandgap ($E_g$) of the samples, the linear portions of the curves that approach zero absorption values are extrapolated. The values of optical bandgap ($E_g$) are recorded in Table 1. It was observed that the calculated values of $E_g$ decrease with the addition of sulfa drag. The decrease in the optical band gap observed in the doped samples can be ascribed to the formation of localized states, referred to as trapping centers, and changes in the degree of disorder. The hydrogen bonding interactions between the PVA and sulfa drug molecules, both inter- and intramolecular, may also play a significant role in this phenomenon.

The extinction coefficient (k) indicates how well the prepared samples absorb light. It is related to the intensities of the absorption bands, indicating the number and strength of chromophores like the carbonyl and hydroxyl groups. The extinction coefficient (k) is calculated from the relation between absorbance coefficient (α) and wavelength (λ) as [33]:

$$\kappa = \frac{\alpha\lambda}{4\pi} \qquad (3)$$

Figure 6 depicts the relationship between the extinction coefficients (k) and the energy (E=hυ).

Due to the dominant absorption behavior at longer wavelengths, the extinction coefficient (k) reaches its maximum value in this region. Moreover, the k values decrease in the UV range as the wavelength increases, eventually reaching steady values close to zero in the visible region. This increase in k values indicates that allows electromagnetic waves to pass through with minimal decay or damping in the visible range. The observed increase in the k value is attributed to the development or reduction of optical absorption of the doped samples.

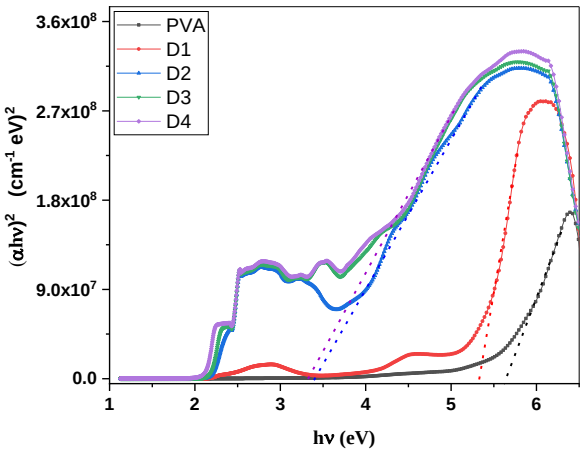


**Figure 4:** The plot between $(\alpha h\upsilon)^2$ versus hυ for PVA/Sulfa drug.

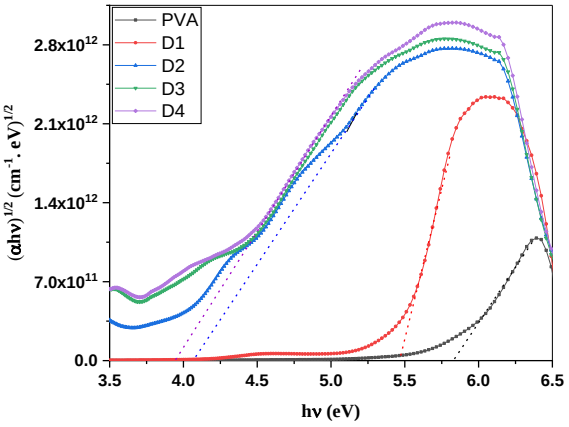


**Figure 5:** The plot between $(\alpha h\upsilon)^{1/2}$ versus hυ for PVA/Sulfa drug.

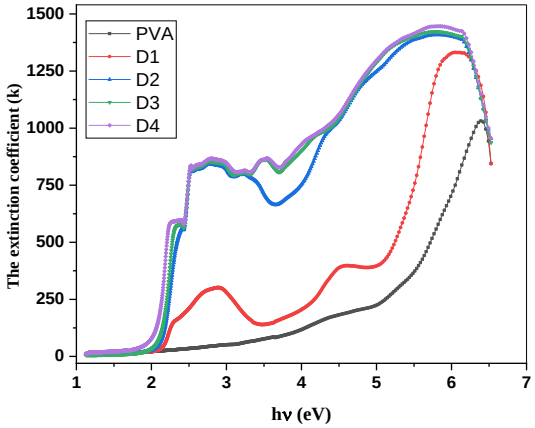


**Figure 6:** The relationship between the extinction coefficients (k) and the energy (E=hυ).

Density functional theory (DFT) was also used to optimize the model structures of the PVA-doped sulfa drug. Gaussian 09 software (Gaussian, Inc., Wallingford, CT, USA) was used to study the electronic properties of synthesized composite material. HOMO/LUMO bandgap energy was also investigated to compare the experimental and theoretical data to approve the reaction mechanism between components and to ensure the final structure. Figure (7) introduces optimized structures in addition to 3D HOMO/LUMO distribution of the sulfa drug, PVA, and their composite materials

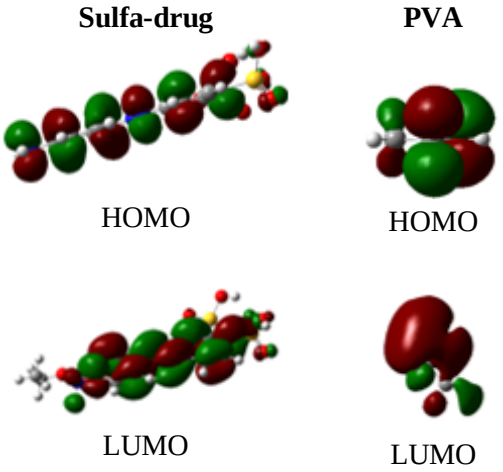


HOMO- Composite material

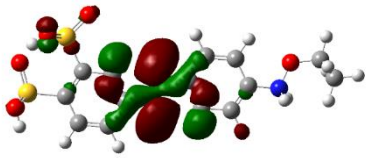

LUMO- Composite material

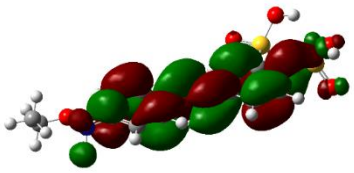

**Figure 7:** optimized structures in addition to 3D HOMO/LUMO distribution of the sulfa drug, PVA, and their composite materials

Obtained data was found to be in agreement with that reported for PVA [34], Sulfa Drugs [35], and hence for their suggested composite structure and approve hydrogen bonding processes [36].

**Table 1:** The values of the direct and indirect energy gap of PVA/Sulfa drug.

| Samples | Direct energy band gap (ev) | Indirect energy band gap (ev) |
|---|---|---|
| PVA | 5.71 | 5.71 |
| D1 | 5.31 | 5.42 |
| D2 | 3.27 | 3.93 |
| D3 | 3.19 | 3.82 |
| D4 | 3.17 | 3.81 |

### 3.3. Antibacterial study against pathogenic grams

Antibacterial activity of studied samples against pathogenic *Methicillin-resistant Staphylococcus aureus* (*MRSA*), *Staphylococcus aureus* (*S. aureus*), *Escherichia coli* (*E-coil*), and *Klebsiella pneumonia* (*K*) was performed using disc agar diffusion method.

Table (2) summarize the inhibitory activity that was determined based on the diameter of the distinct inhibition zone [37, 38].

**Table 2:** Diameter of the inhibition zone (D) and Activity index (Q) against antibiotic (AB) Ciprofloxacin

| | ***MRSA*** | | ***S. aureus*** | | ***E-coil*** | | ***K*** | |
|---|---|---|---|---|---|---|---|---|
| | **D** | **A** | **D** | **A** | **D** | **A** | **D** | **A** |
| **D1** | 6 | 32 | 6.0 | 35 | 5.5 | 34 | 5.5 | 55 |
| **D2** | 6.5 | 35 | 7.0 | 41 | 6.5 | 40 | 6.0 | 60 |

| | | | | | | | | |
|---|---|---|---|---|---|---|---|---|
| **D3** | 7 | 37 | 7.5 | 44 | 7.5 | 46 | 7.0 | 70 |
| **D4** | 7.5 | 40 | 8.5 | 50 | 8.5 | 53 | 8.0 | 80 |
| **AB** | **18** | **100** | **17** | **100** | **16** | **100** | **10** | **100** |

As shown in Table 2, all studied samples revealed a greater level of antimicrobial suppression due to the creation of structural building blocks from the condensation of carboxylic acid groups. The increased antibacterial activity of the composite material may be attributable to strongly positive electrostatic interactions between the charged molecule and the negatively charged cell surface.

## 4. Conclusion

This study aims to carry out the synthesis, characterization, and physicochemical characteristics of PVA-dopped sulphonamide-vitamin C. The morphology and surface properties of the films can be analyzed using scanning electron microscopy (SEM) and atomic force microscope (AFM). The FT-IR absorption spectra of pure PVA polymer show characteristic bands related to the functional groups present in the polymer matrix. The UV-Vis spectroscopy of the PVA films containing the drug has induced significant changes in the optical absorption characteristics of the material, making it a noteworthy example of a benzene-sulfanilamide. The pure PVA polymer displays characteristic bands related to its functional groups in its FT-IR absorption spectrum. The addition of sulfa drug reduces calculated $E_g$ values from 5.71 eV to 3.27 eV. Trapping centers and disorder changes in doped samples cause an optical band gap decrease. PVA-sulfa drug hydrogen bonding contributes to this effect. The higher antimicrobial activity of composite material is attributed to the highly positive electrostatic interactions between the charged molecule and the cell surface that had been negatively charged. It was noticed that sample D3 whichcontains about 0.02 wt% of the drug, can be considered an eco-friendly sample that nearly gives the same physicochemical properties and antibacterial activity similar to that of higher concentrations.

**References**


1. Kango, S., Kalia, S., Celli, A., Njuguna, J., Habibi, Y., Kumar, R., and Alkhuraiji, A. (2021). Polyvinyl alcohol: a versatile polymer for biomedical and beyond applications. Progress in Polymer Science, 112, 101316.
2. Zhang, X., Li, L., Zhang, H., and Zhang, W. (2021). Recent advances in polyvinyl alcohol-based materials for biomedical applications. Journal of Materials Chemistry B, 9(18), 3591-3609.
3. Raza, Z. A., Abbas, N., and Ali, M. (2021). Polyvinyl Alcohol (PVA)-Based Hydrogels: Synthesis, Properties, and Biomedical Applications. In Hydrogels-Based Biomaterials for Advanced Medical and Biomedical Applications (pp. 83-107). Woodhead Publishing.
4. Singh, S., Kumar, R., and Sharma, G. (2020). Polyvinyl alcohol-sulfadiazine hydrogel film as a potential wound dressing material: in vitro and in vivo studies. Journal of Materials Science: Materials in Medicine, 31(3), 24.
5. Nesrinne, A., and Fatima, Z. (2021). Polyvinyl Alcohol/sulfadiazine wound dressings: Synthesis, characterization and drug release studies. Polymer Bulletin, 78(8), 4409-4425.
6. Han, X., Liu, Y., Liu, Y., Wang, G., and Huang, X. (2020). Preparation and characterization of polyvinyl alcohol/sulfadiazine composite nanofiber membranes for wound dressing. Journal of Nanoscience and Nanotechnology, 20(7), 4091-4097.
7. Makhija, D. T., Pokharkar, V. B., and Patil, V. B. (2019). Development and evaluation of sulfamethoxazole and trimethoprim loaded polyvinyl alcohol (PVA) films for wound healing applications. Journal of Drug Delivery Science and Technology, 52, 664-672.
8. Venkatesan, P., and Manavalan, R. (2021). Investigation of release kinetics of sulfadiazine drug from PVA films using UV-visible spectroscopy. Journal of Applied Polymer Science, 138(3), 49798.
9. Wang, J., Yuan, Y. Q., Chen, J. W., and Zhou, X. (2021). Sulfonamide resistance genes in aquatic environments: Occurrence, abundance, and ecological risk. Environment International, 157, 106810.
10. Lee, S. Y., and Lee, J. S. (2021). Sulfonamide antibiotics in the environment: occurrence, fate, and ecological implications. Journal of Hazardous Materials, 417, 125966.
11. Aminov, R. I. (2017). A brief history of the antibiotic era: lessons learned and challenges for the future. Frontiers in microbiology, 8, 1340.
12. Collier, P. J., and Williams, P. N. (2017). The rise of antibiotics in food animals and the emergence of methicillin-resistant Staphylococcus aureus and extended-spectrum beta-lactamase–producing bacteria in humans. Clinical Infectious Diseases, 65(3), 529-536.
13. Spellberg, B., and Gilbert, D. N. (2014). The future of antibiotics and resistance. New England Journal of Medicine, 371(25), 2468-2473.
14. Ventola, C. L. (2015). The antibiotic resistance crisis: part 1: causes and threats. Pharmacy and Therapeutics, 40(4), 277-283.

15. Alharbi, A. F., Alharbi, S. A., Alqarawi, A. A., and Aljarbou, A. N. (2022). Sulfonamides antibiotics: recent advances, applications, and future perspectives. Antibiotics, 11(1), 2.
16. Tamma, P. D., and Doi, Y. (2021). Antibiotic stewardship interventions in the intensive care unit. Infectious Disease Clinics, 35(4), 859-874.
17. Jie Zhou, Xiao Yun, Jiting Wang, Qi Li, and Yanli Wang (2022). A review on the ecotoxicological effect of sulphonamides on aquatic organisms, Toxicol Reports, 9: 534–540.
18. Kumar, S., Kumar, R., and Sharma, G. (2018). Optimization of polyvinyl alcohol-sulfadiazine hydrogel film for wound dressing applications using response surface methodology. Journal of Applied Polymer Science, 135(14), 46146.
19. Thakur, A., Kumar, R., and Sharma, G. (2018). Optimization of physicochemical properties of PVA-sulfadiazine hydrogel film for wound dressing applications using response surface methodology. Journal of Applied Polymer Science, 135(44), 46861.
20. Makhija, D. T., Pokharkar, V. B., and Patil, V. B. (2020). Development and optimization of sulfamethoxazole and trimethoprim loaded polyvinyl alcohol (PVA) films for wound healing applications. Journal of Drug Delivery Science and Technology, 57, 101641.
21. Kumbhar, S., and Bankar, A. (2021). Optimization of physicochemical properties of sulfadiazine and silver sulfadiazine loaded PVA films for wound healing applications. Journal of Drug Delivery Science and Technology, 65, 102756.
22. Makhija, D. T., Pokharkar, V. B., and Patil, V. B. (2021). Development of sulfamethoxazole and trimethoprim loaded polyvinyl alcohol (PVA) films for wound healing applications: optimization using central composite design. Journal of Drug Delivery Science and Technology, 66, 102870.
23. Rajendran, R., and Devi, S. (2019). Optimization and characterization of polyvinyl alcohol-sulfamethoxazole composite films for wound healing applications. Journal of Applied Polymer Science, 136(38), 47819.
24. Ramesh, B., and Kumar, K. S. (2019). Evaluation of the release profile of sulfadiazine from PVA films using FTIR spectroscopy and mathematical modeling. Materials Today: Proceedings, 16, 1824-1830.
25. Venkatesan, P., and Manavalan, R. (2021). Investigation of release kinetics of sulfadiazine drug from PVA films using UV-visible spectroscopy. Journal of Applied Polymer Science, 138(3), 49798.
26. Song, J., Gao, J., Yang, Y., Zhao, X., and Li, J. (2018). Preparation and characterization of polyvinyl alcohol/hydroxyapatite composite nanofiber membranes for guided bone regeneration. Journal of Materials Science: Materials in Medicine, 29(8), 113.
27. Alizadeh, O., and Mirzadeh, H. (2018). Synthesis and characterization of electrospun PVA/Chitosan blend nanofibrous scaffold functionalized with N, S-codoped TiO2 as an efficient visible-light photocatalyst. Applied Surface Science, 444, 311-319.
28. Li, Y., Chen, Y., Wang, Y., and Li, C. (2020). Polyvinyl alcohol hydrogel prepared by freeze-thawing and its application in electronic skin. Journal of Materials Science: Materials in Electronics, 31(7), 4982-4991.
29. Alqurshi, A., Hamid, A. A., and Alhazmi, H. A. (2021). Polyvinyl alcohol/sulfadiazine hydrogel film for wound healing: preparation, characterization and antibacterial activity. Journal of Molecular Liquids, 336, 116431.
30. Hamedi, S., Mottaghitalab, F., Haghighat, S., and Amoabediny, G. (2019). Fabrication and characterization of PVA/SA hydrogel incorporated with carnosine for wound healing applications. Materials Science and Engineering: C, 100, 263-273.
31. Rastogi, S. K., and Singh, S. K. (2019). A review on recent advances in polymer electrolytes for lithium-ion batteries. Polymer-Plastics Technology and Engineering, 58(4), 349-371.
32. Li, H., Li, Y., Zhang, Y., and Chen, T. (2022). Theoretical and experimental investigation of the optical properties of the transparent PVA/Ag nanocomposite films. Journal of Materials Science: Materials in Electronics, 33(1), 90-96.
33. Wu, P., and Brand, L. (1994). Resonance energy transfer: methods and applications. Analytical Biochemistry, 218(1), 1-13.
34. Ahmed, H., & Hashim, A. (2021). Geometryoptimization, optical and electronic characteristics of novel PVA/PEO/SiC structure for electronics applications. Silicon, 13(8), 2639-2644.
35. Alyar, S., Alyar, H., Özmen, Ü. Ö., Aktaş, O., & Erdem, K. (2023). Biochemical properties of Schiff Bases derived from FDA-approved Sulfa drugs: Synthesis, ADME/Molecular Docking studies, and anticancer activity. Journal of Molecular Structure, 136167.
36. Elashmawi, I. S., Abdelghany, A. M., & Hakeem, N. A. (2013). Quantum confinement effect of CdS nanoparticles dispersed within PVP/PVA nanocomposites. Journal of Materials Science: Materials in Electronics, 24, 2956-2961.
37. Abdelghany, A. M., Menazea, A. A., & Ismail, A. M. (2019). Synthesis, characterization and antimicrobial activity of Chitosan/Polyvinyl Alcohol blend doped with Hibiscus Sabdariffa L. extract. Journal of Molecular Structure, 1197, 603-609.
38. Abdelghany, A. M., & Behairy, A. (2020). Optical parameters, antibacterial characteristics and structure correlation of copper ions in cadmium borate glasses. Journal of Materials Research and Technology, 9(5), 10491-10497.